

Atomic Force Microscopy of Protein Complexes

Olga I. Kiselyova and Igor V. Yaminsky

1. Introduction

Scanning probe microscopy (SPM) is a rather new family of surface studies methods, having broad applications to biomedical science. The main advantage of SPM over conventional microscopic techniques (i.e., scanning and transmission electron microscopy) is its ability to study living objects in their natural environment and, therefore, the ability to observe dynamical processes occurring to them with subnanometer resolution. Here, we will discuss one of its family members, atomic force microscopy (AFM), which has yielded fascinating results for the past decade.

AFM is a surface science technique and, thus, requires the immobilization of the studied object on a flat rigid support (substrate). A crystalline microtip attached to a cantilever is brought in contact with the investigated surface. The deflection of the cantilever is roughly proportional to the force of interaction between the tip and the surface. It can be registered by the deflection of a laser beam directed to the reflective surface of the cantilever. The electronic system maintains the constant force value, whereas the cantilever is scanning over the sample. Registration of the cantilever position normal to the sample gives the 3D surface profile. In the dynamical (or resonance) regime of registration the cantilever oscillates near the surface and the amplitude is modulated by the tip-sample interaction force. The surface profile roughly coincides with the surface of equal oscillation amplitude. (For detailed description of the AFM technique, *see refs. 1 and 2*). Probe microscopy technique does not necessarily involve the sample-light interaction and, therefore, the $\lambda/2$ restriction on resolution is removed.

Although AFM can attain the atomic resolution on inorganic crystals, on biological objects it is up to date restricted to molecular one. For that reason,

From: *Methods in Molecular Biology*, vol. 242: *Atomic Force Microscopy: Biomedical Methods and Applications*
Edited by: P. C. Braga and D. Ricci © Humana Press Inc., Totowa, NJ

the main fields of AFM morphological studies of proteins is the formation of nucleic acid–protein and protein–protein complexes, oligomerization, and the organization of protein molecules in biological membranes and Langmuir films (for review, *see* **ref. 3**).

Here, for an example of AFM observation of the protein oligomerization and complex formation, we reproduce the experiments in a system of membrane proteins (cytochrome P450–cytochrome P450 NADH-reductase), which we had previously reported (**4**) and give detailed explanations of the experimental procedure and data interpretation.

2. Materials

1. AFM with tapping mode regime (e.g. Nanoscope, Digital Instruments).
2. Cantilevers (e.g., Nanoprobe, MicroMash).
3. Liquid cell for tapping mode.
4. Supports: highly oriented pyrolytical graphite (HOPG), mica.
5. Protein solution.
6. Tridistilled water.
7. Buffers for the protein under consideration.
8. Double-sided adhesive tape.
9. Metal discs.
10. Filter paper.

3. Methods

The cornerstone of successful imaging by AFM is a proper sample preparation, which can be considered as a sort of art. Preparation technique includes the correct choice of the substrate for immobilization, the adjustment of specimen concentration and buffer ionic strength, drying conditions (if necessary).

3.1. Choosing the Substrate

The main properties a good substrate should possess is flatness (a monocrystal plane would be ideal), rigidity and the studied objects' high adhesion to it. The choice of the substrate material is usually guided by the a priori information about the object's properties. Moreover, for biological research it is favorable to have a set of substrates with different hydrophobicity and surface charge of different sign. Comparing the images of the same object fixed on substrates with hydrophilic and hydrophobic surfaces one can reveal its surface properties. The strength of adhesion and the distribution on the substrate show whether the object's surface is polar, hydrophobic, or positively/negatively charged. This information is of special importance in complex formation studies, indicating which parts of molecules are in contact with each other, and which, with the solvent.

In biological SPM research, two substrates are the most widely used and are the simplest to handle: HOPG and mica. These two materials do not require any preliminary cleaning because simple cleavage (using tweezers or adhesive tape) yields atomically flat crystalline planes of considerable area (tens and hundreds of square microns) practically devoid of defects. Subsequent cleavage of the used plate allows reusing it many times.

HOPG has hydrophobic neutral surface, composed of flat terraces separated by steps. After anodization, the HOPG surface becomes hydrophilic and can be used for covalent binding of proteins (**Note 1**; refs. 5–7).

The surface of mica is, on the contrary, polar, negatively charged, and has high adhesion to many biological specimens. Unfortunately for microscopists, a material with similar properties, but with positively charged surface, has not been found yet. To recharge mica surface, a variety of procedures has been elaborated. The simplest are based on divalent cationic treatment (8,9), others imply more complicated lipid monolayer application (10,11), or one of the most progressive techniques of silanization (12,13). Polypeptide coating produces rough surface and can be used for visualization of whole cells or organelles (14,15). Description of other possible substrates, such as silicon wafers (16), evaporated gold films (17), and Au(111) facets (18), can be found elsewhere (**Note 2**).

3.2. Applying the Sample

The visualization of proteins requires special attention to be paid to the application of material onto the substrate and to related aspects of the sample purity and possible contamination artifacts. The two main techniques of application of protein molecules onto the substrate are direct adsorption and Langmuir film transformation. The latter technique, having certain advantages for amphiphilic molecules, for example membrane proteins, is described elsewhere (19,20). Covalent binding of the proteins to previously applied lipid films or silanized surfaces is specimen specific and requires a detailed description, which can be found elsewhere (21,22). Electrochemical deposition (23) and covalent binding (5) of protein molecules onto anodized HOPG surface are used mainly in scanning tunneling microscopy.

The direct adsorption technique implies, as can be understood from its name, a direct application of the protein solution droplet (several microliters) onto the prepared substrate. Then it is left to adsorb for several minutes, after which the unbound material is rinsed by the same buffer as containing the protein. The exact time of exposition depends on the protein concentration and the adhesion rate and should be adjusted experimentally. Typically used protein concentrations range between 1 $\mu\text{g/mL}$ and 1 mg/mL . After adsorption the

researcher has two choices: to place the sample into the liquid cell of the microscope, add more buffer if necessary and start *in situ* imaging or to dry the sample first and image in air.

Although the second choice does not profit all the AFM potential, it is much easier to perform, and we can recommend it to beginners or as a first step of the experiment. Dried material better adheres to the substrate and cantilever tuning is much easier as well. After drying of the buffer solution, all contaminants and salts containing the drop bulk remain on the surface, sophisticating the objects' identification. Working in liquid facilitates this problem, but on the other hand decreases adhesion stability of the molecules on the substrate. For that reason, before drying, the samples are rinsed with distilled water. The remaining water can be removed by the airflow, then contaminants of the solution will also leave the surface.

Despite all that precautions artifacts are quite often registered in AFM images of the adsorbed proteins, obtained both in liquid and air. Typically, these artifacts are all images of residual contaminants and have the shape of protrusion 3–5 nm in diameter and can be easily mistaken for protein molecules themselves. It is usually the height of the artifacts (1 nm and less) that allows one to distinguish them from the adsorbed protein molecules (**Note 3**).

3.3. AFM Imaging

AFM measurements start with cantilever tuning. In tapping mode lateral tip-sample forces are minimized, which helps to avoid sweeping of the adsorbed material by the tip during scanning. Contact mode silicon nitride cantilevers (Nanoprobe) with a force constant of 0.3–0.6 N/m or Ultrasharp cantilevers of NSC17 series (MicroMash, Estonia) give reliable results for tapping mode imaging of protein molecules in liquid. Samples dried in airflow can be imaged with NanoSensors tapping mode etched silicon probes or cantilevers from noncontact series produced by other manufacturers. The set of parameters is individual for each system. The oscillation amplitude depends on the cantilever's resonant properties. The amplitude of free resonant oscillations A_0 can be chosen between 10 and 50 nm. The aspect ratio of loaded vs free oscillation amplitude A_S/A_0 should be kept in the interval of 0.8–0.9 for air imaging and 0.90–0.95 for imaging in liquid.

Scan rates in tapping mode are relatively low (1–3 Hz, depending on the field size). For imaging individual protein molecules, it is recommended to get several $2 \times 2 \mu\text{m}^2$ images first (to get the idea of coverage density and choose an appropriate area) and then proceed to more detailed $0.5 \times 0.5 \mu\text{m}^2$ ones (**Note 4**; ref. 24).

3.4. Image Interpretation

In SPM the interpretation of images is a key role task, more complicated than obtaining the images. The registered objects are not “labeled” and it is normally their shape and size that serves as criterion to distinguish between them.

It is well established that apparent lateral dimensions of all AFM-imaged objects are overestimated as a result of the influence of the geometry of the probe tip, that has finite size, typically 5–10 nm, that is, the same order that a protein molecule. This can be illustrated by a simple geometrical example (**Fig. 1A**; **ref. 25**).

$$d = 2\sqrt{r^2 + 2Rr}$$

Here, we roughly consider a protein molecule as a sphere with radius r and the probe having a spherical tip with radius R . The depicted trajectory of the tip during scanning and thus the image profile has bell-like shape. Evidently, the apparent diameter d measured at half height does not coincide with the real diameter of the molecule. A real cross-section profile taken from the AFM image of a protein molecule (cytochrome P450) is shown in **Fig. 1B**. Simple geometrical calculations yield the formula for this “tip-broadening” effect.

Knowing the tip radius R one can estimate the real diameter of molecule D

$$D = 2r = 2(\sqrt{R^2 + d^2/4} - R)$$

In practice, the tip is not an ideal sphere of radius R , and its dimensions are usually not known precisely and differ from tip to tip. Moreover, real molecules are not spherical and can be deformed, which makes the above-mentioned calculations very approximate. For this reason, single objects’ lateral dimensions are seldom used in analytical measurements, whereas vertical dimensions are preferable in calculations. A more complicated model of elliptical sample is described elsewhere (**26**).

A successful AFM image of adsorbed globular protein molecules is a set of dots (*see Fig. 2*). Assuming the protein does not oligomerize and the shape is roughly spherical, the dots are round and of equal size. The histogram of height distribution shows a single peak (**Fig. 3A**). In this article we will use the molecules height, measured on the cross-section made along the scan line (*see Fig. 1B* for example of cross-section). Apparent diameter measured at half height, D , can be used for general description or rough estimation of the lateral dimensions. If the molecules are spherical, the peak is very narrow, because all the molecules are identical. If the shape is asymmetric, the peak is widened. The

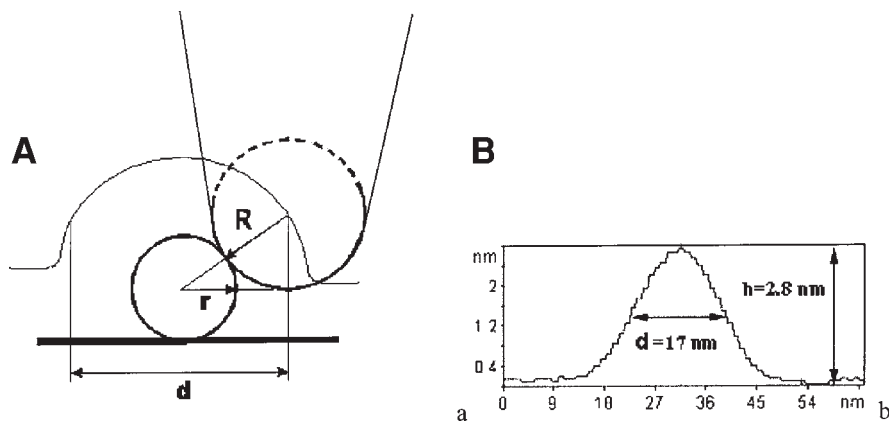


Fig. 1. (A) Illustration of the tip-broadening effect resulting from the tip geometry. R , tip radius; r , molecule radius; d , apparent molecule diameter. (B) A real cross-section profile taken from the AFM image of a protein molecule (cytochrome P450).

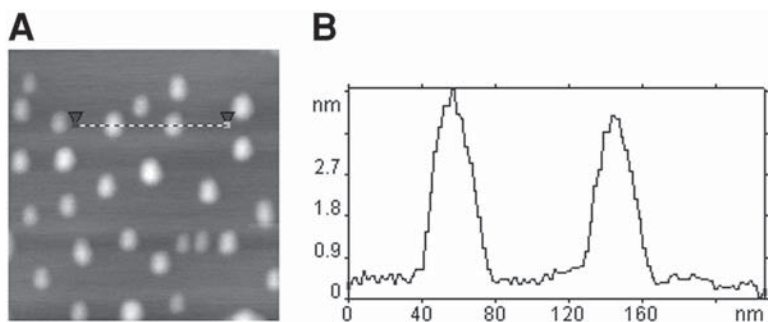


Fig. 2. Molecules of Fp in monomer form adsorbed on HOPG surface (A). Image size $0.3 \times 0.3 \mu\text{m}^2$; (B) cross-section made along the marked line in (A).

molecules can adhere to the substrate with different sites, and therefore, different parts contribute to the height measurements (*see Fig. 4*).

If the asymmetry is considerable, for example one deals with dimers composed of two spherical globules, the histogram might show several peaks (27). Comparing the relative heights of the peaks one can calculate the probability of adsorption on this or that part and the free energy of binding (Note 5).

When transmembranous proteins are extracted from their native membrane surrounding, their molecules form oligomers. The investigation of oligomerization and protein complexes formation by X-ray and diffraction methods is problematic because it requires crystallization of the sample. Meanwhile, the

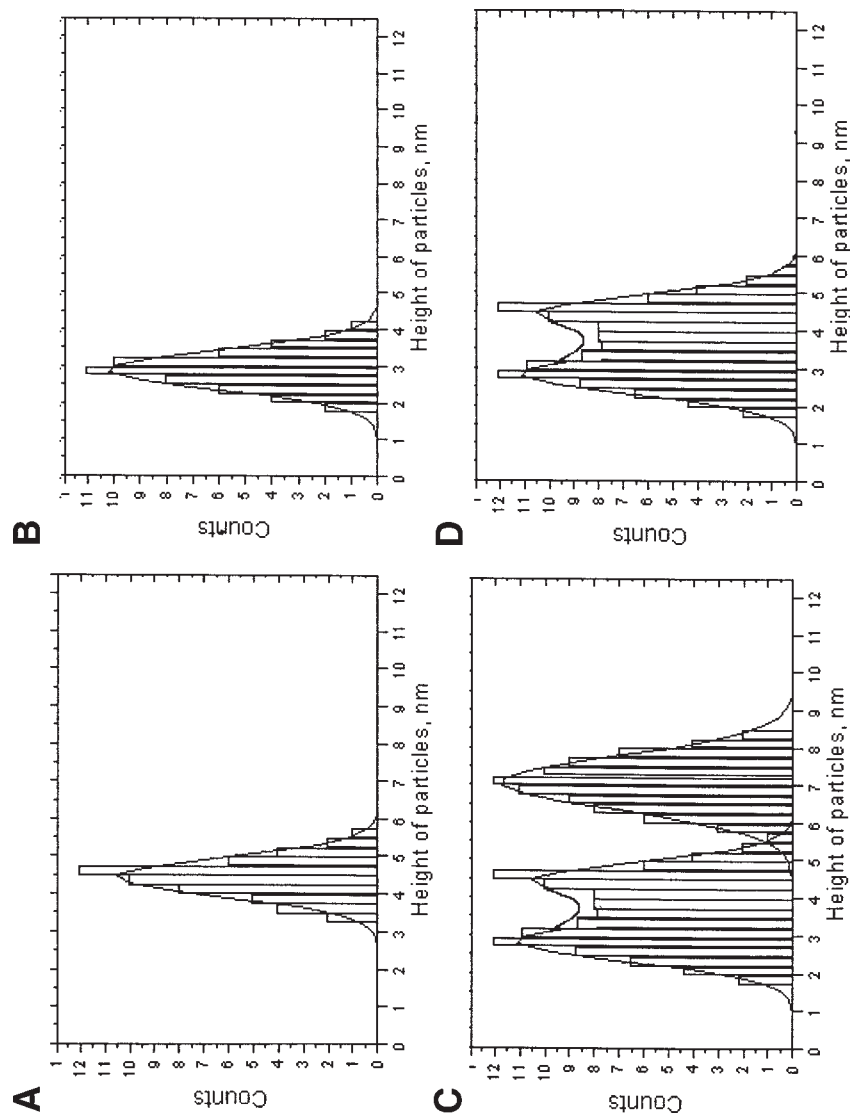


Fig. 3. Histograms of heights distribution of adsorbed proteins. (A) Fp; (B) cytochrome P450; (C) mixture of Fp and cytochrome P450; (D) mixture of noninteracting proteins.

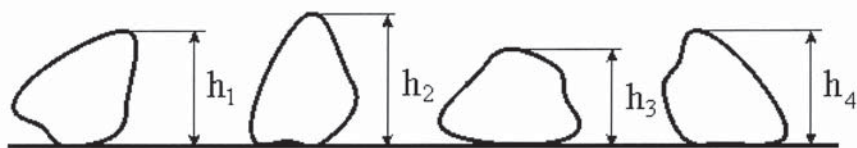


Fig. 4. Possible orientation of a protein molecule adsorbed on a flat substrate.

crystallization of transmembrane proteins is one of the most difficult crystallographic tasks.

In this chapter we describe the results on AFM studies of oligomerization and complex formation for the system of two membrane proteins: cytochrome P450 2B4 (28) and NADPH–cytochrome P450 reductase (Fp) from rabbit liver (29). These proteins are part of the microsomal monooxygenase system, playing the key role in the metabolism of drugs, cancerogenes, mutagens, and xenobiotics. Both proteins oligomerize when extracted from microsomal membranes (30,31).

AFM demonstrates the efficiency of the monomerization procedure previously described (4) for these proteins. **Fig. 2** depicting individual Fp molecules adsorbed on HOPG is a typical example of AFM image of adsorbed protein in monomer form. The distribution of heights is reflected by the histogram (**Fig. 3A**). The height of the molecules is 4–5 nm, the apparent diameter d is 20–22 nm. The histogram consists of a single peak, which indicates that one is dealing with one sort of particles. In order to confirm the fact that Fp is in the monomer form, one should compare the obtained dimensions with independent data. Despite the lack of crystallographic data, the average radius of a protein globule r in Angströms can be roughly estimated using a simple formula for spherical molecules cited by (19):

$$r = 0.717 M^{1/3},$$

where M is the protein's molecular weight in Daltons.

For the Fp with molecular weight of 60 kDa, it yields $r = 2.8$ nm. Therefore, the expectation for the average height in AFM image is 5.6 nm. The registered value of 4.5 nm is quite close. The experimental value of height may be underestimated due to the deformation, caused by the tip's pressure (32). Thus, we can be sure that the obtained image demonstrates Fp monomers. Following the same procedure, the AFM image of cytochrome P450 2B4 on HOPG can be obtained (data not shown). The overall appearance of most globular proteins AFM images is very similar and the measurements of heights are necessary for their sizes evaluation. Height distribution histogram for cytochrome P450 is presented in **Fig. 3B** (**Note 6**).

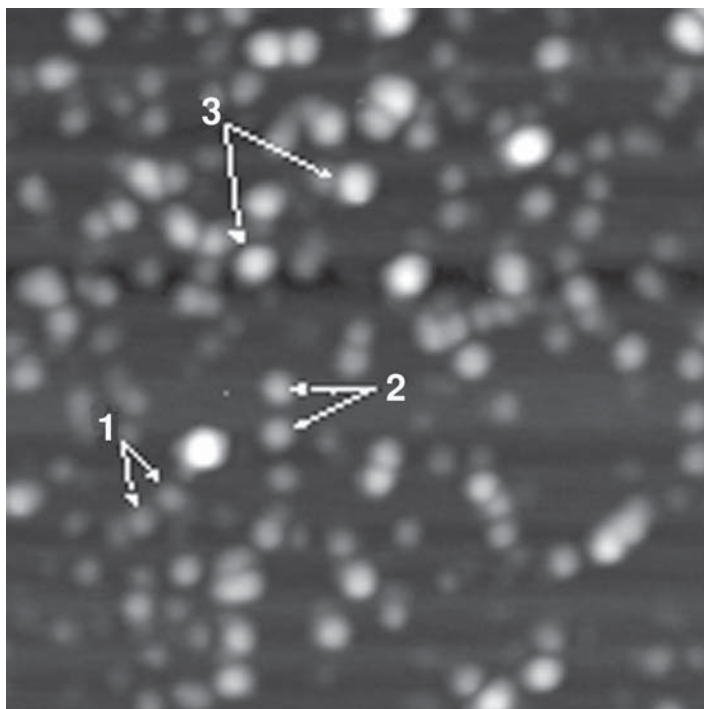


Fig. 5. Mixture of Fp and cytochrome P450 molecules in monomer form adsorbed on mica surface. Image size $540 \times 540 \text{ nm}^2$. Arrows indicate: 1, cytochrome P450; 2, cytochrome P450 NADPH-reductase (Fp); 3, complexes of cytochrome P450 2B4 with Fp (P450/Fp).

Complexes of cytochrome P450 2B4 and NADPH-cytochrome P450 reductase (2B4/Fp) were obtained by mixing respective solutions of monomer proteins of the same molar concentrations. After the incubation, the mixture was diluted and applied onto the substrate.

The AFM image of the mixture applied onto mica substrate is depicted in **Fig. 5**. The image represents a variety of dots of different sizes, which visually seem chaotic. Because the initial mixture contained Fp monomers and cytochrome P450 monomers, the AFM image can represent those and, possibly, the product of their interaction, that is, complexes. The identification of the observed particles is based on the heights distribution.

The histogram of heights' distribution consists of three peaks (**Fig. 3C**). The position of the first peak (2.5–3.0 nm) coincides with that of the peak at the histogram for cytochrome P450 2B4 (**Fig. 3B**), that is, it represents cytochrome P450 2B4 monomers. The second one (the height of 4–5 nm) corresponds to

Fp monomers (compare with **Fig. 3A**). If the two proteins did not interact, the histogram of the mixture would be the sum of the two independent ones and would contain two peaks (**Fig. 3D**). But the experimental histogram (**Fig. 3C**) shows the third peak, located at 6–8 nm, corresponding to complexes of cytochrome P450 2B4 and NADPH-cytochrome P450 reductase (2B4/Fp). The molecules of cytochrome P450, Fp, and 2B4/Fp are indicated by arrows with respective numbers in **Fig. 5**.

Using the technique described above, one can investigate the oligomerization of each of the two proteins in the absence of detergent and qualitatively reveal the dependency of the oligomerization percent versus the protein concentration and buffer ionic strength. AFM image of the oligomers of cytochrome P450 (**Fig. 6A**) is apparently similar to that of P450/Fp mixture. Individual monomers within oligomers are not resolved. For the estimation of oligomers percentage one can make height distribution histograms and determine the size of oligomers (**Fig. 6B**; **Note 7**). Determination of the number of particles in each oligomer requires a geometrical model. The choice of the model depends on the ratio of sizes and *a priori* knowledge of the molecule properties.

4. Notes

1. If steps are not seen in the image of $10 \times 10 \mu\text{m}^2$, either the user is very lucky to have an extremely high quality material, or the feedback system of the microscope is not working properly). When using HOPG one has to be careful about artifacts, which are now well established (**6,7**).
2. Because long contact with the atmosphere contaminates the substrate surface, cleavage should be performed right before the application of the sample. Before using a certain substrate for a biological experiment it is strongly recommended to get a few images of it to check for possible defects and artifacts.
3. It is strongly recommended to get several control AFM images of the buffer solution used (using the preparation technique described above) and compare them to protein molecules images, in order to reveal possible contamination artifacts. Much attention should be paid to the purity of water and chemicals.
4. It is important to bear in mind that A_0 and A_s/A_0 parameters might influence the apparent height of the biological objects imaged, introducing up to 15% error (for details, see **ref. 24**). Therefore, for analytical measurements it is recommended to use the same parameters for images one is going to compare. Using the same cantilever would be the best.
5. If the tip happens to be asymmetric, the AFM image of a spherical particle reflects the tip's shape and can be triangle, elliptical, or other. If so, the orientation of the figure is the same for all particles registered in the field. It is recommended to rotate the sample manually and see if the pattern rotates, too. If it is due to the

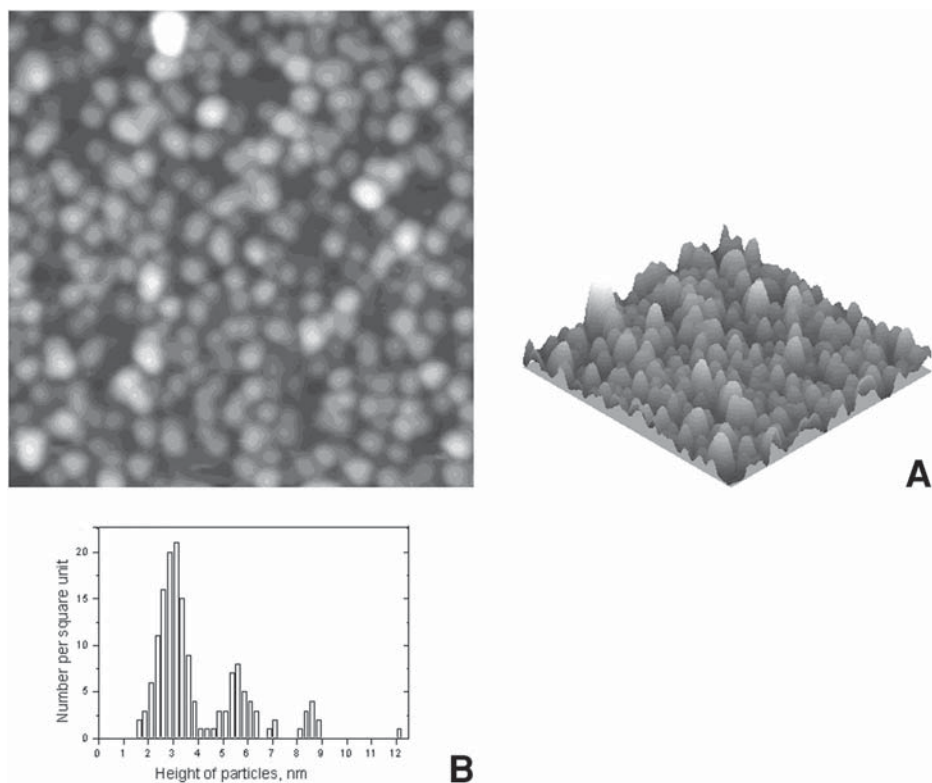


Fig. 6. (A) Molecules of cytochrome P450 in oligomer form adsorbed on mica surface, 2D and 3D images, respectively. Image size is $480 \times 480 \text{ nm}^2$. (B) Histogram of height distribution shows three peaks. The first (approx 3 nm) corresponds to monomers, the second (approx 5.5 nm) and the third (8.5 nm), presumably octamers and 12–30-mers, respectively.

- tip's asymmetry, the orientation of figures does not change.
- Here and further in that chapter we imaged dried samples. Such an approach is justified because the monomer–oligomer state is believed not to change upon drying. Detergents containing in the buffer often produce foam, and the bubbles do not allow imaging with a microscope with light detection of cantilever position.
 - The two proteins and their complex may have different adsorption rate to the substrate used. Therefore, one has to be careful when using the height of peaks at the histogram for the estimation of the relative part of complexes formed. If such estimations are really essential, it is recommended to calculate the amount of single molecules of one of the proteins and compare it to that adsorbed from this protein solution of the same concentration on the same area. The difference will indicate the amount, forming the complex.

Acknowledgments

This work was supported by INTAS (grant no. 01-0045), Russian Foundation for Basic Research (Grant nos. 00-04-55020 and Russian Ministry of Science and Technology (Grant no. 40.012.1.1.1151).

References

1. Binnig, G., Quate, C. F., and Gerber, Ch. (1986) Atomic force microscope. *Phys. Rev. Lett.* **56**, 930–933.
2. Meyer, G., and Amer, N. M. (1988) Novel optical approach to atomic force microscopy. *Appl. Phys. Lett.* **53**, 1045–1047.
3. Kiselyova, O. I., and Yaminsky, I. V. (1999) Proteins and membrane-protein complexes. *Colloid J.* **61**, 1–19.
4. Kiselyova, O. I., Yaminsky, I. V., Ivanov, Yu., D., Kanaeva, I. P., Kuznetsov, V. Yu., et al. (1999) Study of membrane proteins, cytochrome P450 2B4, and NADPH-cytochrome P450 reductase and their complex formation. *Arch. Biochem. Biophys.* **371**, 1–7.
5. Zhang, J., Chi, Q., Dong, S., and Wang, E. (1996) In situ electrochemical scanning tunneling microscopy investigation of structure for horseradish peroxidase and its electrocatalytic property. *Biochem. Bioenergetics* **39**, 267–274.
6. Chang, H. and Bard, A. J. (1991) Observation and characterization by scanning tunneling microscopy of structures generated by cleaving highly oriented pyrolytic graphite. *Langmuir* **7**, 1143–1153.
7. Dunlap, D. D. and Bustamante, C. (1989) Images of single-stranded nucleic acids by scanning tunneling microscopy. *Nature* **324**, 204–206.
8. Bustamante, C., Vesenska, J., Tang, C. L., Lees, W., Guthhold, M., and Keller, R. (1992) Circular DNA molecules imaged in air by scanning force microscopy. *Biochemistry* **31**, 22–26.
9. Vesenska, J., Guthhold, M., Tang, C. L., Keller, R., Delaine, E., and Bustamante, C. (1992) Substrate preparation for reliable imaging of DNA molecules with the scanning force microscope. *Ultramicroscopy* **42–44**, 1243–1249.
10. Onishi, S., Hara, M., Furuno, T., Okada, T., and Sasabe, H. (1993) Direct visualization of polypeptide shell of ferritin molecule by atomic force microscopy. *Biophys. J.* **65**, 573–577.
11. Kacher, C. M., Weiss, I. M., Stewart, R. J., Schmidt, C. F., Hansma, P. K., Radmacher, M., et al. (2000) Imaging microtubules and kinesin decorated microtubules using tapping mode atomic force microscopy in fluids. *Eur. Biophys. J.* **28**, 611–620.
12. Lyubchenko, Yu., L., Shlyakhtenko, L. S., Harrington, R. E., Oden, P. I., and Lindsay, S. M. (1993) Atomic force microscopy of long DNA: Imaging in air and under water. *Proc. Natl. Acad. Sci. USA* **90**, 2137–2140.
13. Shlyakhtenko, L. S., Potaman, V. N., Sinden, R. R., and Lyubchenko, Yu, L. (1998) Structure and dynamics of supercoil-stabilized DNA cruciforms. *J. Mol. Biol.* **280**, 61–72.

14. Bolshakova, A. V., Kiselyova, O. I., Filonov, A. S., Frolova, O., Yu., Lyubchenko, Y. L., and Yaminsky, I. V. (2001) Comparative studies of bacteria with atomic force microscopy operating in different modes. *Ultramicroscopy* **68**, 121–128.
15. Vater, W., Fritzsche, W., Schaper, A., Bohm, K. J., Unger, E., and Jovin, T. M. (1995) Scanning force microscopy of microtubules and polymorphic tubulin assemblies in air and in liquid. *J. Cell Sci.* **108**, 1063–1069.
16. Mazeran, P.-E., Loubet, J.-L., Martelet, C., and Theretz, A. (1995) Under buffer SFM observation of immunospecies adsorbed on a cyano grafted silicon substrate. *Ultramicroscopy* **60**, 33–40.
17. Andersen, J. E. T., Moller, P., Pedersen, M. V., and Ulstrup, J. (1995) Cytochrome c dynamics at gold and glassy carbon surfaces monitored by in situ scanning tunnel microscopy. *Surface Sci.* **325**, 193–205.
18. Leggett, G. J., Davies, M. C., Jackson, D. E., Roberts, C. J., Tendler, S. J. B., and Williams, P. M. (1993) Studies of covalently immobilized protein molecules by scanning tunneling microscopy: The role of water in image contrast formation *J. Phys. Chem.* **97**, 8852–8854.
19. Guryev, O. L., Dubrovsky, T., Chernogolov, A., Dubrovskaya, S., Usanov, S., and Nicolini, C. (1997) Orientation of cytochrome P450_{scc} in Langmuir-Blodgett monolayers. *Langmuir* **13**, 299–304.
20. Kiselyova, O. I., Guryev, O. L., Krivosheev, A. V., Usanov, S. A., and Yaminsky, I. V. (1999) Atomic force microscopy studies of Langmuir-Blodgett films of cytochrome P450 scc (CYP11J1): Hemoprotein aggregation states and interaction with lipids. *Langmuir* **15**, 1353–1359.
21. Weisenhorn, A. L., Drake, B., Prater, C. B., Gould, S. A. C., Hansma, P. K., Ohnesorge, F., et al. (1990) Immobilized proteins in buffer solution at molecular resolution by atomic force microscopy. *Biophys. J.* **58**, 1251–1258.
22. Karrasch, S., Hegerl, R., Hoh, J. H., Baumeister, W., and Engel, A. (1994) Atomic force microscopy produces faithful high-resolution images of protein surfaces in an aqueous environment. *Proc. Natl. Acad. Sci. USA.* **91**, 836–838.
23. Zhang, J., Chi, Q., Dong, S., and Wang, E. (1995) STM of folded and unfolded haemoglobin molecules electrochemically deposited on highly oriented pyrolytic graphite. *J. Chem. Soc. Faraday Trans.* **91**, 1471–1475.
24. Kiselyova, O. I., Galyamov, M. O., Nasikan, N. S., Yaminsky, I. V., Karpova, O. V., and Novikov, V. K. (2002) Scanning probe microscopy of biomacromolecules: nucleic acids, proteins and their complexes, in *Frontiers of Multifunctional Nanosystems* (Buzanaeva, E. V., and Scharff, P., eds.), Kluwer Academic Publishers, Dordrecht, pp. 321–330.
25. Stemmer, A. and Engel, A. (1990) Imaging biological macromolecules by STM: quantitative interpretation of topographs. *Ultramicroscopy* **34**, 129–140.
26. Gallyamov, M. O., and Yaminskii, I. V. (2001) Quantitative methods for restoration of true topographical properties of objects using the measured AFM-images. 2. The effect of broadening of the AFM-profile. *Surface Invest.* **16**, 1135–1141.
27. Waner, M. J., Gilchrist, M., Schindler, M., and Dantus, M. (1998) Imaging the molecular dimensions and oligomerization of proteins at liquid/solid interfaces. *J. Phys. Chem. B.* **102**, 1649–1657.

28. Imai, Y., Hashimoto, Y. C., Satake, H., Garardin, A., and Sato, R. (1980) Multiple forms of cytochrome P450 purified from liver microsomes of phenobarbital- and 3-methylcholantrene-pretreated rabbits. *J. Biochem.* **88**, 489–503.
29. Kanaeva, I. P., Skotselyas, E. D., Kuznetsova, G. P., Antonova, G. N., Bachmanova, G. I., and Archakov A. I. (1985) Reconstruction of a membrane monooxygenase cytochrome P 450-containing system in the liver using detergents in solution. *Biokhimia* **50**, 1382–138.
30. Dean, W. L. and Gray, R. D. (1982) Relationship between state of aggregation and catalytic activity for cytochrome P-450LM2 and NADPH-cytochrome P-450 reductase. *J. Biol. Chem.* **257**, 14679–14695.
31. Wagner, S. L., Dean, W. L., and Gray, R. D. (1984) Effect of a zwitterionic detergent on the state of aggregation and catalytic activity of cytochrome P-450LM2 and NADPH-cytochrome P-450 reductase. *J. Biol. Chem.* **259**, 2390–2395.
32. Gallyamov, M. O. and Yaminsky, I. V. (2001) Quantitative methods of restoration of true topographical properties of the objects by measurement of AFM-images. 1. Contact deformations of the probe and the specimen. *Surface Invest.* **16**, 1127–1134.